



Somatostatin therapy, neprilysin activation, and amyloid beta reduction: A novel approach for Alzheimer's treatment

Nicole G. Metzendorf^{a,*}, Ana Godec^a, Alex Petrovic^a, Aikaterini Chourlia^a, Antonino Napoleone^a, Stina Syvänen^b, Fadi Rofo^a, Greta Hultqvist^{a,*}

^a Department of Pharmacy, Uppsala University, Husargatan 3, Box 580, Uppsala 751 23, Sweden

^b Department of Public Health and Caring Sciences, Uppsala University, Uppsala, Sweden

ARTICLE INFO

Keywords:

Neprilysin
Somatostatin
SST
MME
Transferrin receptor
TfR
Blood brain barrier
BBB
Alzheimer's disease
Degradation
Amyloid beta
Transport
Protein pharmaceuticals
Biologicals
Aggregation
Oligomers
Hairpin
A11

ABSTRACT

Introduction: Neprilysin is the primary enzyme responsible for the degradation of amyloid beta (A β), with its levels regulated by the hormone somatostatin (SST).

Methods: We have developed a novel treatment mechanism for Alzheimer's disease (AD) by combining SST with a blood-brain barrier (BBB) transporter and a Fc fragment to extend its half-life. This treatment was tested in a murine AD model overexpressing amyloid precursor protein (APP) with the Arctic mutation in A β (APP^{ArcSwe}).
Results: Our findings demonstrate a significant increase in neprilysin levels, which correlates with a reduction in various forms of A β , including membrane-bound and intracellular A β aggregates, as well as A β 42 in insoluble aggregates.

Discussion: These results suggest that neprilysin can effectively degrade A β with the Arctic mutation. Additionally, this treatment strategy successfully reduces both oligomeric and larger A β aggregates, a challenge for other therapeutic approaches. This novel strategy holds promise as a potential therapeutic approach for AD.

1. Introduction

In Alzheimer's disease (AD), when the concentration of the endogenous amyloid beta (A β) peptide becomes too high, it begins to aggregate, ultimately leading to the onset of the disease. A β peptide is generated through the cleavage of amyloid precursor protein (APP) by secretases. APP is synthesized in the cytosol and then transported axonally in vesicles to the presynaptic terminals, but not post-synapses. During this transport, beta and gamma-secretase cleave APP to form A β [1]. To maintain steady A β levels, it is either cleared from the brain or degraded. In sporadic AD, which accounts for 98 % of cases, reduced A β degradation is commonly observed [2–4].

The main protease responsible for A β degradation is neprilysin [5–9]. Neprilysin is a 90–110 kDa metallopeptidase protein that is exclusively expressed in neurons in the brain. After synthesis in the

soma, it is axonally transported to the presynaptic terminals [10], similar to APP transport. Neprilysin expression in the brain is highly selective, with high levels in regions such as the hippocampus, but very low expression in other areas of the brain [11,12]. Notably, these regions with high neprilysin expression are the regions first affected by AD. Neprilysin is also expressed in other parts of the body, such as the gastrointestinal tract. It cleaves both membrane-associated A β [12,13] and A β in solution. Neprilysin knockout mice show increased A β burden, reduced hippocampal synaptic plasticity, and cognitive impairment [14, 15]. In humans with AD, neprilysin levels are significantly reduced in areas with A β pathology [16,17]. Studies in aging mice have shown that neprilysin levels can decrease by as much as 83 % in the regions most effected by AD [18]. In line with findings in the human AD brain, transgenic mice with A β aggregates also exhibit decreased neprilysin levels in brain regions most affected by A β aggregates, such as the

* Corresponding authors.

E-mail addresses: Nicole.Metzendorf@uu.se (N.G. Metzendorf), Greta.Hultqvist@uu.se (G. Hultqvist).

<https://doi.org/10.1016/j.bioph.2025.118325>

Received 15 April 2025; Received in revised form 30 June 2025; Accepted 2 July 2025

Available online 8 July 2025

0753-3322/© 2025 The Author(s). Published by Elsevier Masson SAS. This is an open access article under the CC BY license (<http://creativecommons.org/licenses/by/4.0/>).

hippocampus. However, in regions with less A β accumulation, neprilysin levels remain unchanged.

The monomeric A β peptide is an intrinsically disordered protein (IDP), meaning it lacks a stable, folded structure and remains flexible. One of the conformations it adopts is a beta hairpin, a structural feature thought to be an early step in the aggregation process [19]. The beta hairpin is believed to be a precursor to larger aggregates, and studies suggest that A β trimers containing this beta hairpin could represent some of the smallest, and potentially most toxic, forms of aggregates. These small aggregates, particularly those formed by A β 42, are considered key contributors to the neurotoxic effects associated with AD, as they can disrupt cellular functions and contribute to neurodegeneration [19,20].

One of the familiar variants of AD is the Arctic mutation in the A β peptide. The amyloid beta produced by the mice used in this study carries the Arctic mutation. This mutation involves a single amino acid substitution, glutamic acid (E) to glycine (G) at position 22 of A β (E22G), also known as E693G in the amyloid precursor protein (APP). It was first identified in a family in northern Sweden, which is why it is referred to as the Arctic mutation. This mutation has a significant impact on the A β peptide as it accelerates the aggregation of A β compared to the wild-type form. However, the aggregates formed by the Arctic mutation are less compact than those of wild-type A β . These aggregates are often referred to as protofibrils, which are intermediate structures in the aggregation process. Protofibrils are thought to be more flexible and structurally disordered, often exposing hydrophobic regions that disrupt cell membranes. Therefore these protofibrils are believed to be more toxic than larger, more stable fibrils, as they can disrupt cellular function, trigger oxidative stress and contribute to the neurodegenerative processes in AD [21].

The cyclic peptide somatostatin (SST) has been demonstrated to significantly enhance neprilysin activity by increasing both intracellular and membrane-bound neprilysin levels, potentially making the enzyme more active as well [12,22]. Research has shown that SST expression is notably reduced in AD [23,24], which could contribute to the pathophysiology of the disease. While small molecule binders to somatostatin receptor (SSTRs) are available, their clinical utility is limited due to poor blood-brain barrier (BBB) penetration and very short half-lives, making them less effective for targeting the brain in the context of AD treatment [25] [26,27].

Using proteins or peptides as therapeutics for brain diseases is challenging due to the BBB, which effectively prevents larger molecules from entering the brain. To overcome this hurdle, we and others have successfully utilized the transferrin receptor (TfR) system to actively transport larger protein therapeutics in to the brain [28–31]. This is achieved by incorporating a TfR-binding domain into the therapeutic protein, allowing it to cross the BBB and reach its target in the brain, thus enhancing the potential for effective treatment of neurological conditions.

We have previously shown that an SST peptide attached to a TfR-targeting BBB transporter can double the levels and activity of neprilysin in the hippocampus and reduce the levels of membrane-bound A β in the same region in the APP_{Swe} model, which overexpresses wild-type A β [12,32]. Furthermore, it has been reported that neprilysin is unable to degrade A β containing mutations that increase the aggregation speed, such as the Arctic mutation [33]. However, we have recently demonstrated that soluble neprilysin can indeed degrade Arctic A β and is even more efficient in degrading Arctic A β than wild-type A β [34]. This finding is significant, as it suggests that neprilysin may be a viable therapeutic target for treating Alzheimer's disease, even in the presence of mutations that cause more rapid A β aggregation.

Fc domains of an IgG antibodies are known to substantially enhance blood half-life of protein constructs. Here, we have fused a single-chain variant of an IgG Fc (scFc) we previously designed [35], to the SST peptide with the TfR targeting BBB transporter to further extend the half-life of the protein drug. This construct, SST-scFc-scFv8D3, was then

tested in the APP_{ArcSwe} mouse model, which not only carries the Swedish mutation but also has the Arctic mutation. We observed that the addition of the scFc extension significantly extends the half-life of the construct. Furthermore, a single injection of the novel protein drug resulted in a significant upregulation of neprilysin levels in the hippocampus. It also led to a reduction in A β 42 levels in both the membrane-bound and non-soluble components of the brain, as well as a decrease in A β oligomers containing hairpins in the membrane-bound part of the hippocampal region. These results confirm that neprilysin can effectively degrade A β with the Arctic mutation. Additionally, this study suggests that increasing neprilysin levels could be a promising future treatment strategy, not only for targeting extracellular A β but also for addressing intracellular and membrane-bound A β aggregates, which have been more challenging to target with other treatments.

2. Results

2.1. Construct design and production

The constructs SST-scFc-scFv8D3, scFc-scFv8D3, and scFc (Fig. 1A) were transiently expressed in Expi293 cells and purified using protein G affinity chromatography. The protein yield was approx. 3–6 mg per liter of cell culture. Purity and molecular weight of the proteins were assessed by SDS-PAGE, confirming estimated molecular weights consistent with expected constructs SST-scFc-scFv8D3 (MW = 85.5 kDa), scFc-scFv8D3 (MW = 83.9 kDa), and scFc (MW = 53.8 kDa). All three proteins exhibited a purity of approximately 90 % based on densitometric analysis of Coomassie-stained gels (Fig. 1B). Additional quality assessments were performed using thermal shift stability analysis (Supplementary Figure 1B), which indicated that the recombinant proteins possess high structural stability.

2.2. Retained TfR binding of the designed constructs

To confirm that the SST-scFc-scFv8D3 protein retained its ability to bind to the TfR, we performed a TfR-specific ELISA. The binding curve showed similar affinity to TfR as reported previously [12,28,36] (Fig. 1C). Additionally, we used mass photometry to analyze whether the proteins were monomeric or if multimers had formed. The mass photometry analysis revealed that SST-scFc-scFv8D3, along with the control proteins scFc-scFv8D3 and scFc were predominantly present as monomers, with only a minor fraction (approx. 4 %) existing as dimers for SST-scFc-scFv8D3 (Supplementary Figure 1). This was further supported by dynamic light scattering analysis (Supplementary Figure 1 C).

2.3. The SST constructs can increase the levels of neprilysin in SHSY5Y cells

The addition of the large scFc and the BBB transporter to the SST peptide could potentially affect its functionality. To assess this, we evaluated its functionality in vitro using a neprilysin activation assay in SHSY5Y cells, where the different constructs were added to the cell media. We confirmed that all constructs were equally effective in enhancing neprilysin activity as SST alone (Fig. 1D). The control construct scFc-scFv8D3, which does not contain SST, also slightly increased neprilysin levels. However, this increase was likely due to a rise in cell numbers rather than an enhancement of neprilysin activity, as previously observed with scFv8D3 [12].

2.4. SST-scFc-scFv8D3 enters the brain efficiently in wild-type mice after 2 h

We further aimed to confirm that SST-scFc-scFv8D3 could enter the brain in vivo. Iodine-125 (¹²⁵I) labelled SST-scFc-scFv8D3, scFc-scFv8D3 and scFc were intravenously injected into the tail vein of wild-type (wt) mice at a tracer dose (0.3 nmol/kg, Fig. 2A). Two hours post-

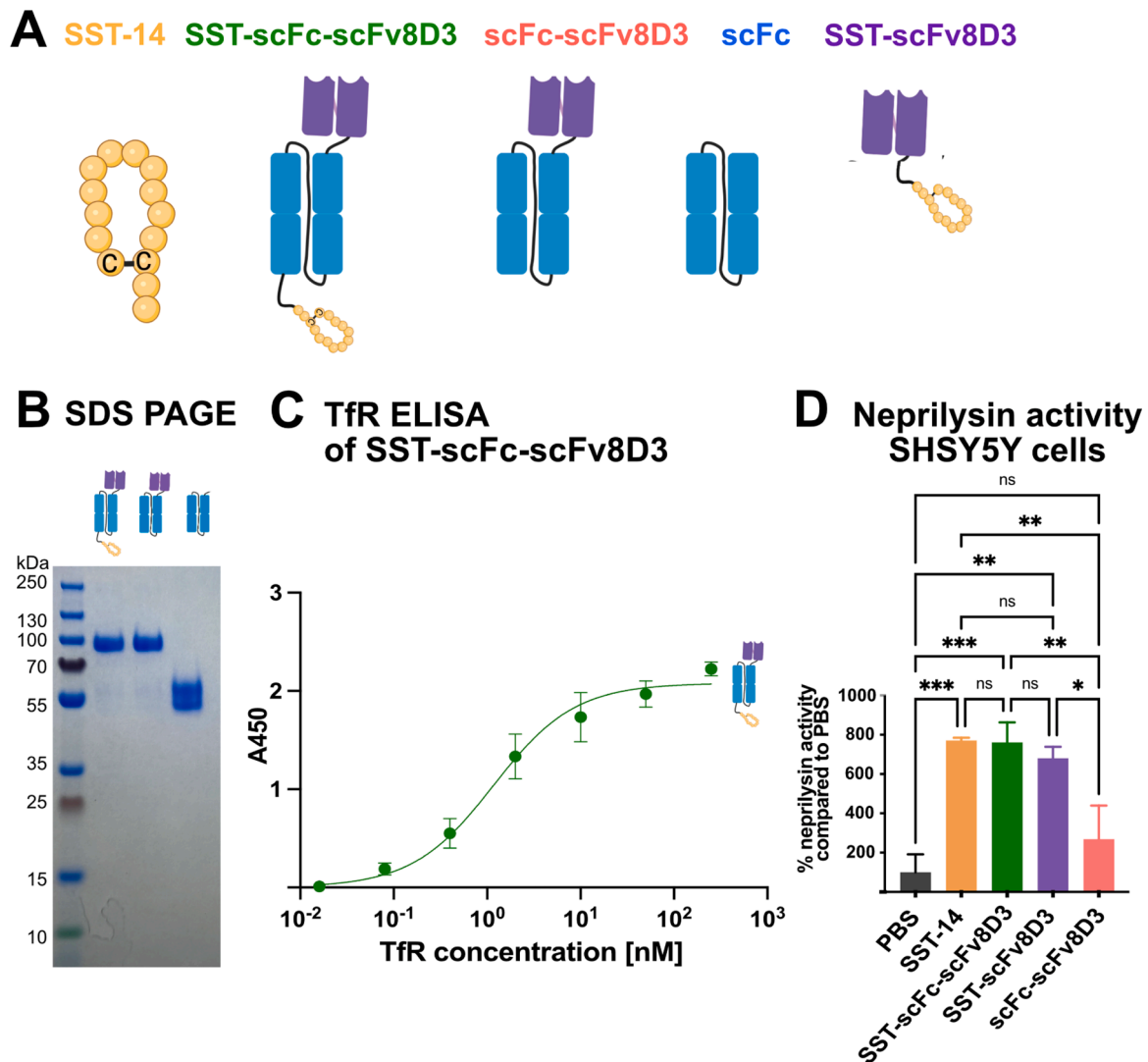


Fig. 1. Design, purification, and functional characterization of SST-scFc-scFv8D3 and control constructs. **A)** Design of SST-scFc-scFv8D3, scFc-scFv8D3 and scFc. Somatostatin-14 (SST-14, SST) is a cyclic peptide with 14 amino acids, circulated by a disulfide bond. In this construct, SST is linked to a single-chain fragment of the constant domain (scFc) from murine IgG2c (shown in blue) and a single-chain-fragment variable (scFv) of the antibody 8D3 (shown in purple), which specifically binds to the transferrin receptor. Control constructs include scFc-scFv8D3 and scFc as controls. **B)** SDS PAGE image of the purified proteins, including SST-scFc-scFv8D3 (MW = 85.5 kDa), scFc-scFv8D3 (MW = 83.9 kDa) and scFc (MW = 53.8 kDa). **C)** Transferrin receptor binding properties of SST-scFc-scFv8D3. An ELISA was performed using the extracellular domain of murine transferrin receptor (TfR), showing that SST-scFc-scFv8D3 binds to TfR. Results are presented as mean \pm SD. **D)** Enhanced neprilysin activity in SHSY5Y cells treated with the different SST constructs. Human SHSY5Y cells were incubated for 24 h with 10 μ M of SST, SST-scFc-scFv8D3, SST-scFv8D3, scFc-scFv8D3, and PBS as a negative control. Both the peptide SST and the recombinant proteins SST-scFc-scFv8D3 and SST-scFv8D3 significantly enhanced the neprilysin activity compared to PBS and the control scFc-scFv8D3. Results are presented as mean \pm SD and analyzed using an unpaired *t*-test (*: $p < 0.05$, **: $p < 0.01$, ***: $p < 0.001$, and ns: $p > 0.05$).

injection, we observed an uptake of approx. 0.5–0.9 % of the injected dose (ID) per gram of brain tissue (Fig. 2B). This was significantly higher than the brain concentrations seen for an antibody lacking the BBB transporter and in a similar range to those reported for TfR-transported protein therapeutics [28,37] (Fig. 2C). It has previously been shown that the BBB transporter enables the therapeutic cargo to cross the brain capillaries and reach the brain parenchyma [36,38].

2.5. In vivo treatment experiment in *APP_{ArcSwe}* mice

To examine whether SST-scFc-scFv8D3 had a therapeutic effect in the *APP_{ArcSwe}* mice, which overexpress A β with the Arctic mutation, we conducted an experimental investigation. A β with the Arctic mutation is known to aggregate more rapidly than the wild-type A β , and previous studies have reported that it is not cleaved by neprilysin [33], contradicting our earlier in vitro observations [34]. To investigate this further,

¹²⁵I-labeled SST-scFc-scFv8D3 and scFc-scFv8D3 (control) were administered at a therapeutic dose of 30 nmol/kg (equivalent to 2.5 mg/kg body weight). Mice were sacrificed by cardiac perfusion 96 h post-injection, and the organs were collected for subsequent analysis (Fig. 2A). This approach aimed to evaluate the therapeutic potential of SST-scFc-scFv8D3, specifically its impact on A β aggregation and clearance in the context of the Arctic mutation.

2.6. Enhanced blood half-life by addition of the scFc

To confirm that the addition of the scFc enhanced the half-life of the construct, blood samples were collected during the 96 h of the experiment described above. The half-life of the constructs containing scFc was at least 45 h, while the construct without scFc had a half-life of approx. 6 h, indicating an 8–10-times increase in half-life with the addition of scFc (Fig. 2C). Biodistribution in other tissues is shown in

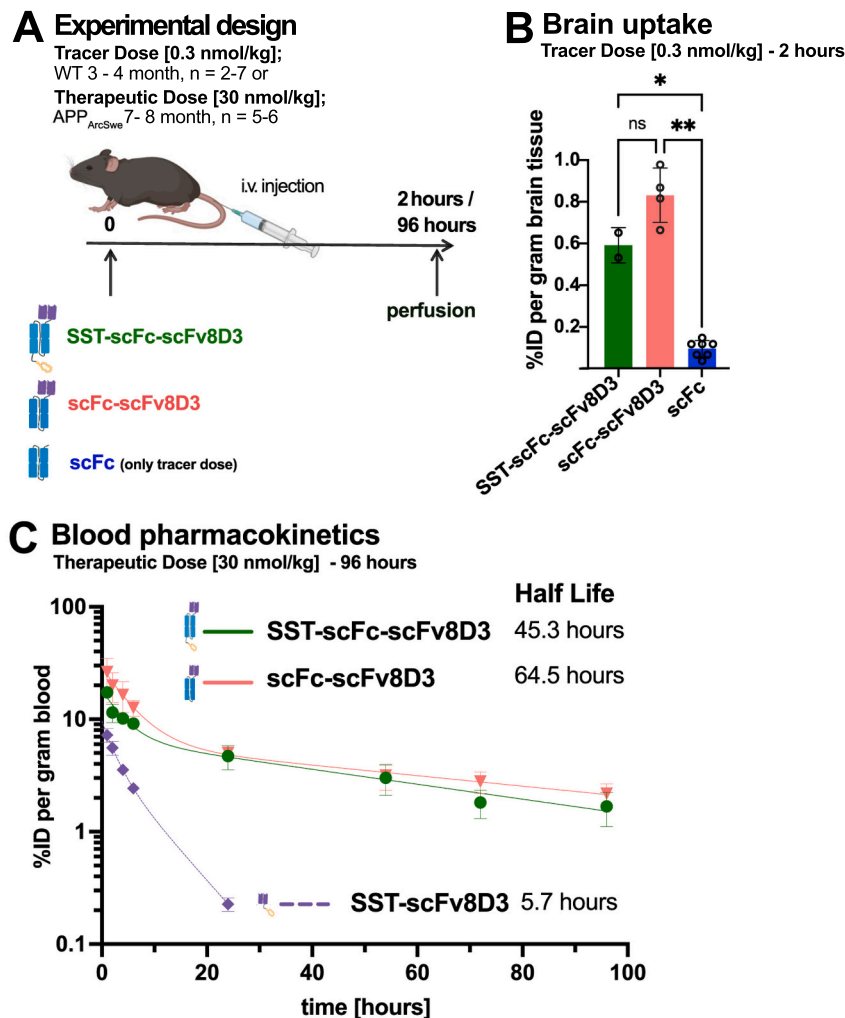


Fig. 2. Brain uptake and blood pharmacokinetics of SST-scFc-scFv8D3. **A) Study design.** Wild-type mice (wt, n = 2–7) were intravenously injected with a tracer dose (0.3 nmol/kg) of [¹²⁵I]SST-scFc-scFv8D3, along with control groups receiving [¹²⁵I]scFc-scFv8D3 and [¹²⁵I]scFc. For blood pharmacokinetics, a therapeutic dose of 30 nmol/kg was intravenously injected into 7–8 month-old APP_{ArcSwe} mice (n = 6 per group), and blood samples were collected over 96 h. **B) Brain uptake.** Brain uptake was measured as percentage of injected dose per gram brain tissue two hours post-injection. Results are presented as mean ± SD and analyzed using an unpaired t test (*: p < 0.05, **: p < 0.01, ***: p < 0.001 and ns: p > 0.05). Data represents n = 2–7 per group. **C) Blood pharmacokinetics.** Blood pharmacokinetics were analyzed for the therapeutic dose (30 nmol/kg) of [¹²⁵I]SST-scFc-scFv8D3, [¹²⁵I]scFc-scFv8D3 and [¹²⁵I]SST-scFv8D3 administered intravenously to 7–8 month-old APP_{ArcSwe} mice (n = 6 per group), were analyzed over 96 h, and the percentage of injected dose per gram blood was determined. The half-life was calculated based on a two-phase-decay calculation. Results are presented as mean ± SD.

Supplementary Figure 2. To confirm the integrity of the [¹²⁵I]-labelled scFc-scFv8D3 and SST-scFc-scFv8D3 proteins are still intact thin layer chromatography (TLC) was performed on plasma samples. The results indicated that the majority of the radiolabelled proteins remained intact, with only trace amounts of the isotope detected (**Supplementary Figure 3**).

2.7. Hippocampal neprilysin levels are increased after in vivo treatment experiment

The left hemisphere of the brain was dissected into three regions (hippocampal area, rest of cerebrum and cerebellum) to assess whether a single injection of SST-scFc-scFv8D3 could increase neprilysin levels in APP_{ArcSwe} mice (**Fig. 3A**). The different brain regions were homogenised in three steps. First, soluble extracellular and cytosolic proteins were isolated using TBS buffer (TBS fraction) without detergent. In the second step, Triton X-100, which dissolves membranes, was added to the remaining pellet after the TBS fraction was isolated. Following centrifugation, the second fraction contained membrane-associated proteins and proteins from some organelles (TBST fraction). The third fraction,

known as the FA fraction, was obtained by using formic acid (FA) to dissolve aggregates (into monomeric form) and other insoluble proteins, which were spun down after the previous steps.

ELISA analysis of neprilysin levels showed that it was predominantly found in the TBST fraction (**Fig. 3B**, TBS fraction **Supplementary Figure 4**), as expected for a membrane-bound protein. The TBST fraction showed a significant increase in neprilysin levels following SST-scFc-scFv8D3 treatment in the hippocampus and the surrounding cortex (**Fig. 3B**). Neprilysin levels in the kidney, where it is also expressed, did not change following SST-scFc-scFv8D3 treatment. (**Fig. 3B**).

2.8. Decreased levels of hippocampal Aβ₄₂ monomers and smaller aggregates in the membrane fraction

Aβ and its various types of aggregates were present in varying amounts across all three fractions obtained during the three-step homogenization. Plaques, insoluble extracellular aggregates, are primarily found in the FA fraction, though some may dissolve during homogenization and appear in other fractions. Monomers are likely to be predominantly present in the soluble TBS fraction. The most toxic Aβ

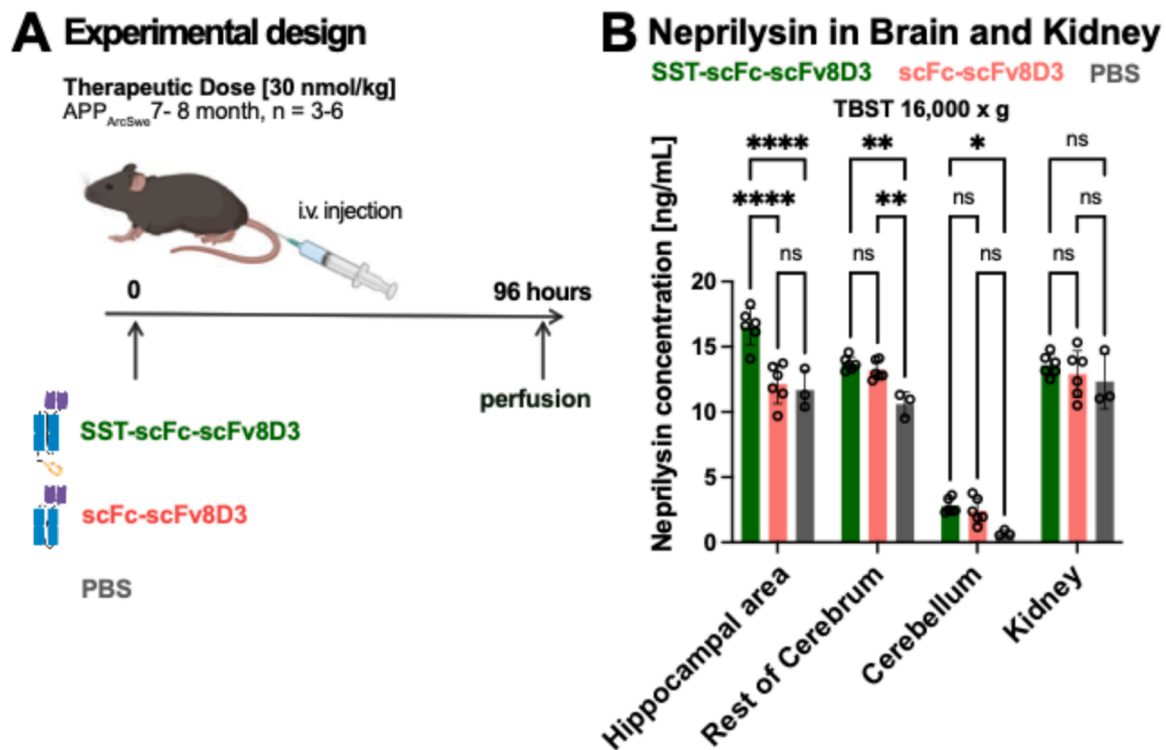


Fig. 3. Neprilysin levels in different brain regions and in the kidney in the membrane fraction after the *in vivo* treatment study. **A.** Study design. For the treatment study, a therapeutic dose of 30 nmol/kg was intravenously injected into 7–8 month-old APP_{ArcSwe} mice (n = 6 per recombinant protein and n = 3 for control group PBS) and euthanized after 96 h. **B.** Neprilysin levels were measured in homogenates from brain regions and kidney (TBST) in 7–8 month-old APP_{ArcSwe} 96 h after a single intravenous injection of 30 nmol/kg (2.5 mg / kg body weight) of [¹²⁵I]SST-scFc-scFv8D3 (n = 6), [¹²⁵I]scFc-scFv8D3 (n = 6) and PBS (n = 3) as a control. Neprilysin levels were quantified using ELISA. Treatment with SST-scFc-scFv8D3 resulted in a significant increase in neprilysin levels in the hippocampal area. No change was detected in kidney TBST homogenates. Results are presented as mean ± SD and analyzed using an unpaired t test (*: p < 0.05, **: p < 0.01, ****: p < 0.0001 and ns: p > 0.05).

aggregates are the small, soluble forms, which are likely present in both the TBS and TBST fractions and may cause more damage when bound to membranes. Detecting various forms of A β in tissue homogenates using ELISAs or similar methods is highly dependent on the assay design [39]. In larger A β aggregates, the C-terminal of the protein is more shielded than the N-terminal, making it less accessible to antibodies across all aggregate types [39] hence using a C-terminal binding antibody will more likely detect smaller A β aggregates and A β oligomers.

96 h after treatment a substantial decrease in A β 42 monomers and aggregates with accessible C- and N-terminal was observed in the TBST fraction (Fig. 4), suggesting that neprilysin can cleave A β with the Arctic mutation. This sandwich ELISA uses an N-terminal A β binding antibody and a C-terminal A β 42 binding antibody [12]. Described in reference [39] as EA β mdopf1–42, the assay requires both the N-terminal and C-terminal regions to be accessible for detection. Thus, it likely detects smaller aggregates and monomers with both ends exposed.

Additionally, we observed a reduction in A β 42 content in the FA fraction in the hippocampal area using the same ELISA set up (Fig. 4). This reduction was evident not only in the hippocampal area but also in the rest of the cerebrum. Since the FA dissolves aggregates to their monomeric forms, this ELISA measures post-mortem-generated A β 42 monomers in the FA fraction, rather than the total amount of A β monomers in the fraction (i.e., not including A β 40 monomers). Therefore, the observed reduction likely reflects changes in A β 42-specific monomers, while the total A β content, including A β 40, remains unaccounted for in this measurement.

2.9. No significant reduction of larger A β aggregates after *in vivo* treatment study

An ELISA using the N-terminal binding antibody 3D6 as both capture and detection antibody detects most types of aggregates, starting from dimers and larger (EA β dopf1-X ELISA in reference [39]). It cannot detect monomers, as they have only one available 3D6 epitope for binding. However, because it binds to an N-terminal epitope, it is more likely to detect larger aggregates compared to antibodies targeting the C-terminal region. In Fig. 5 we used this setup in an ELISA, which shows that these types of aggregates were not altered in our *in vivo* treatment study.

2.10. Detection of A β 42 monomers was not possible and no reduction in total amount of monomers was detected after treatment

Our results suggest that the main decrease in A β is in smaller aggregates with the C-terminal available, likely consisting primarily of A β 42. However, it is unclear whether the difference is due to small A β aggregates or A β 42 monomers. To analyze the monomeric A β , we used the monomer-specific antibody m266 (the murine version of Solanezumab) [40] as a capture antibody, along with various detection antibodies. When using the A β 42 specific antibody for detection, the signals in the ELISA were below the assay's detection limit of the assay and could not be interpreted (data not shown), likely because most of the antibodies was bound by A β 40. Therefore, we cannot confirm whether the levels of A β 42 monomers have decreased. Analysis of A β monomers, which should primarily be A β 40 in this mouse model, showed no differences in signal (Supplementary Figure 5).

2.11. Reduced levels of A β with hairpins which are usually present in smaller aggregates after in vivo treatment study with SST

The reduction of A β after treatment is likely due to a decrease in smaller aggregates. When aggregates begin to form, they initially create a beta hairpin structure, which is lost as the aggregates grow larger and transform into fibrils [19,41,42]. In fibrils, the hairpin is twisted, and beta sheets are formed. The A11 antibody detects the beta hairpin in smaller aggregates but does not bind to larger aggregates without the hairpin [43]. An ELISA using the A11 antibody as a capture antibody showed a decrease in A β with the hairpin structure in the hippocampal area after treatment (Fig. 6, ELISA EA β 01-X in reference [39]).

2.12. The levels of various forms of neprilysin and A β in the plasma after in vivo study

As the SST-scFc-scFv8D3 construct was injected intravenously, it will first distribute in the blood before entering the brain via TfR-mediated transport across the BBB. Since neprilysin levels were only increased in the brain (Fig. 3B) and not in the kidney, we aimed to investigate whether neprilysin and A β levels were affected in the plasma. However, somatostatin receptor levels in the blood are likely low, and neprilysin levels in plasma remained undetectable by ELISA in all treatment groups (data not shown). Our data showed that levels of human A β 40 and A β 42 monomers in plasma were elevated 96 h after SST-scFc-scFv8D3 injection, but no such increase was observed in the control groups (Fig. 7).

3. Discussion

In this study, we developed a novel treatment for Alzheimer's disease (AD) using the hormone SST to enhance endogenous levels, an enzyme that degrades A β . Specifically, we attached a BBB transporter to SST and extended its half-life by incorporating an Fc fragment. This treatment was tested in the APP_{ArcticSwe} mouse model, which overexpresses A β with the Arctic mutation. The results showed increased neprilysin levels in

the hippocampus and a reduction in membrane-associated, intracellular and insoluble A β 42, as well as oligomeric A β .

In Alzheimer's disease, the hippocampus is the first region affected by A β aggregation. In this study, we show that neprilysin levels primarily increase in the hippocampus following treatment. It is also in the hippocampus that we observed the main reduction in specific A β types, particularly membrane-bound A β 42 monomers and aggregates. Since a C-terminal region-binding antibody was used, the detected aggregates are likely smaller, as the C-terminal is often hidden in larger aggregates. These findings are consistent with our earlier work [12] using a mouse model expressing human wild-type A β without the Arctic mutation. Additionally, we observed a reduction in the A β 42 content of insoluble aggregates, which was not analyzed in our previous study. The reduction was observed not only in the hippocampus but also throughout the cerebrum, suggesting a widespread effect of neprilysin in A β 42 levels. No reduction in the A β 40 levels was detected.

Our results suggest that using SST to enhance neprilysin levels primarily facilitates the degradation of A β 42, with a lesser effect on A β 40. Neprilysin has been shown to cleave both A β 40 and A β 42 in vitro, with a greater efficiency for A β 40 [34]. However, extracellular A β 42 is more commonly associated with membranes than A β 40 [44,45], making A β 42 more accessible for cleavage by neprilysin, which is also present in the membrane. This could explain why our in vivo results differ from earlier in vitro results. Additionally, it has been shown that lipids and membranes promote the catalysis of oligomers from A β 42 monomers [44,45]. If neprilysin reduces A β 42 levels near the membrane or intracellularly, it could decrease oligomerization of A β 42 in these locations. A β 42 is more commonly found in the core of A β plaques, while A β 40 is more prevalent in the periphery [46]. Thus, it is possible that A β 40 aggregates extracellularly through association with earlier-formed A β 42 plaque cores. Another potential explanation is that neprilysin could influence the cleavage of APP by gamma secretase, thereby affecting the balance of A β 42 and A β 40 production.

In this study, we also examined the levels of A β containing a hairpin structure, which are likely smaller oligomers or aggregates. Our results

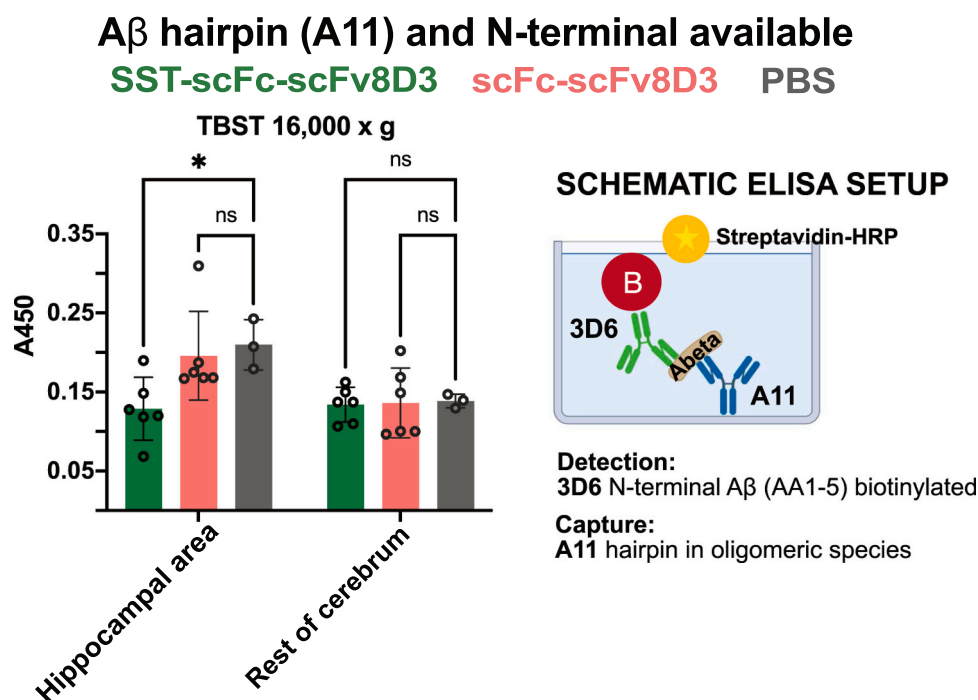


Fig. 6. ELISA analysis of hairpin A β of TBST brain homogenates from the in vivo treatment study with SST-scFc-scFv8D3. This ELISA detects A β with beta in small aggregates with beta hairpin structure and shows a significant reduction in the levels of hairpin A β in the membrane-soluble fraction of the hippocampal region, 96 h post-injection of [¹²⁵I]SST-scFc-scFv8D3 (30 nmol/kg) via a single intravenous injection. Results are presented as mean \pm SD and analyzed using an unpaired t test (*: $p < 0.05$ and ns: $p > 0.05$).

A β 40 and A β 42 monomers in Plasma

SST-scFc-scFv8D3 scFc-scFv8D3 PBS

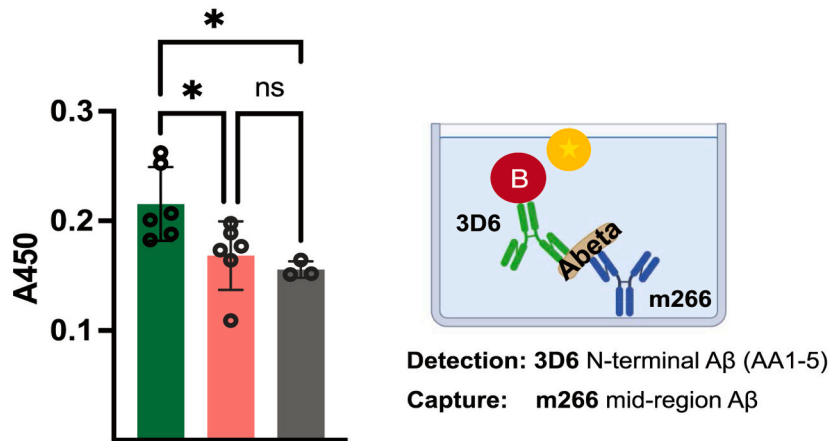


Fig. 7. ELISA analysis of A β 40 and A β 42 monomer levels in plasma after in vivo treatment. Levels of A β 40 and A β 42 monomers were elevated 96 h after a single intravenous injection of [125 I]SST-scFc-scFv8D3 or [125 I]scFc-scFv8D3 (30 nmol/kg) in 7 – 8 month-old APP_{ArcSwe} mice in plasma. Results are presented as mean \pm SD and analyzed using an unpaired t test (*: $p < 0.05$ and ns: $p > 0.05$).

show a reduction of these forms in the hippocampus of SST-scFc-scFv8D3-treated animals. The absence of a reduction in larger soluble aggregates may be to the study design. The treatment was administered over four days, a timeframe during which smaller, more transient aggregates are more likely to be affected, compared to larger, more stable aggregates. It is possible that longer treatment durations could impact larger aggregates as well, but this will need to be explored in future studies.

The reduced levels of specific A β forms in the APP_{ArcSwe} animal model suggest that neprilysin is capable of cleaving A β with the Arctic mutation, a point that has been debated previously. The data presented here supports our earlier in vitro findings, demonstrating that neprilysin efficiently cleaves A β with the Arctic mutation [34]. Neprilysin levels were substantially increased in the hippocampus and only slightly increased in the rest of the cerebrum. Despite this, we observed a decrease in A β 42 levels throughout the cerebrum, suggesting that neprilysin's effect may spread beyond the hippocampus.

Additionally, our results indicate a slight increase of the A β levels in plasma, suggesting that the treatment did not enhance neprilysin levels in the blood. This is an important finding, as an increase in neprilysin in tissues outside the brain could lead to unwanted side effects. It is, of course, possible that the SST may cause side effects that were not detected in these experiments, and this possibility should be studied further.

There is little correlation between plaque load and cognitive function in Alzheimer's disease, whereas a strong correlation exists between the levels of soluble small aggregates and cognition. It is also very likely that intracellular and membrane-bound A β contribute significantly to toxicity, and these forms cannot be targeted by currently clinically approved antibodies. Therefore, treatment strategies aimed at removing intracellular A β , membrane-bound A β and small aggregates are needed. Here, we demonstrate that a treatment using a brain-penetrating SST in a murine model overexpressing human A β with the Arctic mutation increases levels of the A β -degrading enzyme neprilysin, leading to reduced membrane-bound oligomeric A β and A β 42 aggregates. This represents a novel treatment approach with high potential of clinical impacts.

4. Materials and methods

4.1. Design of recombinant proteins

SST-scFc-scFv8D3 was generated by fusing somatostatin (SST, mouse, AGCKNFFWKTFTSC) to the constant region of the heavy chain, as previously described [35]. Briefly, SST was linked to the C-terminus of the constant region of the heavy chain (single-chain fragment constant; scFc) via a linker sequence ("APGSGGAPG"). The scFv8D3 TFR transporter variable region [47], composed of the heavy and light chains, was then connected to the N-terminus of the scFc.

4.2. Expression and purification of proteins

The recombinant proteins SST-scFc-scFv8D3, scFc-scFv8D3, and scFc were expressed in Expi293 cells (cat. no. A14527, Thermo Fisher) and purified using the ÄKTA Start system (Cytiva) and Protein-G columns (cat. no. 17-0405-01, Cytiva) as described previously [28,48]. Briefly, Expi293 cells were transiently transfected with pcDNA3.4 vectors using the transfection reagent polyethylenimine (PEI, cat. no. A14527, Polysciences). The supernatant was harvested after seven days post-transfection, clarified using Cellpure (cat. no. 525243, Sigma-Aldrich), and filtered through a 0.2 μ m PES membrane filter (cat. no. GWP04700, Millipore) before applying to a Protein-G column. Proteins were eluted with 0.7 % acetic acid (cat. no. 33209, Sigma-Aldrich) and subsequently exchanged into PBS (cat. no. 14190250, Thermo Fisher) with 7 K desalting columns (cat. no. 89892, Thermo Scientific). Protein concentration was determined by measuring absorbance at 280 nm.

4.2.1. Confirmation of purity and size by SDS-PAGE

Purified SST-scFc-scFv8D3, scFc-scFv8D3, and scFc were mixed with 25 % LDS sample buffer (cat. no. B0007, Life Technologies), and loaded onto a 4–12 % Bis-Tris protein gel (cat. no. NW04125BOX, Invitrogen). The gel was run at 80 V for analysis and stained with PAGE Blue Protein Staining Solution (cat. no. 24620, Thermo Fisher). Molecular weight was determined by comparing the protein bands to a pre-stained protein ladder (PageRuler™ Plus Prestained Protein Ladder, 10 – 250 kDa; cat. no. 26619, Thermo Scientific). Images were captured using the Odyssey Fc Imaging System (LI-COR Biosciences, Bad Homburg, Germany).

4.2.2. Mass photometry

The purity of the recombinant proteins SST-scFc-scFv8D3, scFc-scFv8D3, and scFc were validated using mass photometry, performed on a Refeyn 2MP System (Refeyn Ltd., Oxford, UK). This method determines the molecular mass by analyzing the proportional relationship between the intensity of light scattering generated by the molecules interacting with the glass surface and their molecular mass [49]. The resulting data are presented as histograms based on mass distribution. Values below zero correspond to buffer impurities, which are neglectable for the proteins analysed in this experiment.

4.2.3. Thermal shift assay

The structural stability of the recombinant proteins was assessed by using the Tycho NT.6 instrument (NanoTemper Technologies GmbH, Munich, Germany) as previously described [12]. Briefly, equimolar concentrations (1 μ M) of the proteins were loaded into glass capillaries (NanoTemper Technologies GmbH, Munich, Germany) and heated from 35°C to 95°C with a linear temperature gradient. The fluorescence intensities at 350 and 330 nm were measured, and the ratio of these intensities was used to calculate the first derivative. The inflection temperature, which corresponds to the peak in the first derivative of the 350 nm / 330 nm ratio, was determined to indicate at which major unfolding events occurs.

4.2.4. Dynamic light scattering

To further assess the quality of the purified proteins, dynamic light scattering (DLS) analysis was performed on SST-scFc-scFv8D3, scFc-scFv8D3, and scFc using an Anton Paar Litesizer 100 (Anton Paar GmbH, Graz, Austria). The size distribution was analysed based on intensity-weighted, on volume-weighted and on number-weighted models. The hydrodynamic diameter was determined using the number weighted-model.

4.2.5. In vitro analysis of binding to the recombinant protein to the mouse transferrin receptor

The binding of the purified SST-scFc-scFv8D3 to the mouse transferrin receptor (TfR) was assessed using a previously described ELISA [29]. Briefly, 50 ng of recombinant mouse TfR in PBS was added to each well of a 96-well half-area plates (cat. no. 3960, Corning Incorporated) and incubated overnight at 4°C. Blocking was performed with 1 % BSA (cat. no. A7030, Sigma-Aldrich) in PBS for two hours at room temperature (RT). Serial dilutions of SST-scFc-scFv8D3 in ELISA incubation buffer (1 x PBS with 0.1 % BSA and 0.05 % Tween-20) were added to the wells and incubated for two hours at RT with shaking. For detection, horse-radish peroxidase (HRP) conjugated goat anti-mouse secondary antibodies (cat. no. 12349, Sigma-Aldrich) was used, followed by signal development with K-blue aqueous TMB (cat. no.331177, Neogen Corp) and an equal amount of 1 M H₂SO₄ (cat. no. 35347, Fisher Scientific) as stopping reagent. Absorbance was measured at 450 nm using a Spark® multimode microplate reader (Tecan, Männedorf, Switzerland). After blocking, the wells were washed with ELISA washing buffer (1 x PBS with 0.05 % Tween-20) between each step.

4.2.6. Cell culture

The human neuroblastoma cell line SHSY5Y was cultured in T75 flasks (cat.no. 83.3911.002, Sarstedt) at 37°C with 5 % CO₂ in a 1:1 (v/v) mixture of minimum essential medium (MEM, cat. no. 41090036, Gibco) and Ham's F-12 medium (cat. no. 21127002, Gibco), supplemented with 10 % fetal bovine serum (FBS, cat. no. 10270106, Gibco). For maintenance, cells were cultured to 80 % confluency, detached with TrypLE (cat. no. 12604013, Gibco) according to manufacturer's instructions, and seeded at a density of approx. 80,000 cells/mL. Cells were plated in 96-well black plates with clear bottoms (cat. no. 3603, Corning Incorporated) at a density of 5000 cells per well.

4.2.7. Neprilysin activity measurement in vitro

The activity of cell-surface neprilysin in SHSY5Y cells was measured as previously described [50]. SHSY5Y cells were starved 48 h prior to the protein treatment by switching to a serum-free medium to eliminate the effect of the serum. The cells were treated with 10 μ M of SST peptide (cat. no. 4032, PeptaNova), SST-scFc-scFv8D3, SST-scFv8D3, or scFc-scFv8D3 for 24 h at 37°C. Cyclo-SST (cat. no. 3493, Tocris) was used as a SSTR antagonist. After the incubation, the media was removed, and the cells were washed with 0.1 M MES (pH 7.0). The cells were then incubated for 1 h at 37°C with a substrate mix containing 0.2 M MES, EDTA-free complete protease inhibitor (cat. no. 05056489001, Roche), Z-LLLaldehyde (final concentration of 1 μ M, cat.no. 3175, Peptide Institute) and Suc-Ala-Ala-Phe-MCA (final concentration of 0.5 mM, cat. no. S8758, Sigma-Aldrich) in assay buffer (50 mM Tris-HCl pH 7.6, 25 mM NaCl, 5 mM ZnCl₂). To inhibit neprilysin activity, thiorphan (final concentration 10 μ M, cat. no. T6031, Sigma-Aldrich) diluted in the assay buffer (50 mM Tris-HCl pH 7.6, 25 mM NaCl, 5 mM ZnCl₂) was added to half of the wells. Phosphoramidon (final concentration 0.1 mM, cat. no. 4052-25, PeptaNova) and leucine aminopeptidase (final concentration 0.1 mg/mL, cat. no. L5006, Sigma) were then added to the wells and incubated for an additional 30 min at 37°C. Fluorescence intensity was measured at excitation 320 nm and emission 410 nm using FLUOstar Omega microplate reader (BMG Labtech, Ortenberg, Germany). Due to limitations of the plate reader, the wavelengths could not be adjusted to the optimal settings for detecting MCA fluorescence (excitation 380 nm and emission at 460 nm), which may have affected the sensitivity of the fluorescence readings. Neprilysin activity was defined by the difference in fluorescence intensity between the thiorphan-negative and thiorphan-positive reactions.

4.2.8. Radiolabelling of recombinant proteins with iodine-125

For in vivo analysis, recombinant proteins were labelled with iodine-125 (¹²⁵I, cat. no. NEZ033A010MC, Revvity) as previously described [51,52]. [¹²⁵I] primarily targets tyrosine and to lesser extent even histidine and tryptophan, provided they are accessible and reactive. Consequently, labelling is not evenly distributed across the entire protein. Labelling was performed by mixing the recombinant protein with 125I in PBS, followed immediately by direct ionization with 1 mg/mL chloramine-T (cat. no. 857319, Sigma-Aldrich) for 90 s at room temperature. The reaction was quenched by adding 1 mg/mL sodium meta-bisulphate (cat. no. 08982, Sigma-Aldrich). To remove free and unbound iodine, the radio-labelled proteins were applied to Zeba mini columns (7 K, cat. no. 89883, Thermo Fisher) for buffer exchange to PBS. The labelling yield ranged from 65 % to 75 %, determined by calculating the activity based on the initial amount of ¹²⁵I added and the remaining activity of the radio-labelled proteins after the buffer exchange. Radiolabelling was always performed one to two hours prior to the experiment. For administration, the ¹²⁵I-labelled recombinant proteins were delivered either as an equimolar tracer dose (0.3 nmol/kg) or equimolar therapeutic dose (30 nmol/kg). For therapeutic dose, only 10 % of the administered dose was labelled with ¹²⁵I, this was mixed with unlabelled recombinant proteins 1:10 (v/v) ratio.

4.2.9. Animals for in vivo study

C57Bl/6J BomTAC mice (n = 10, male, 3–4 months, weight range: 27.2 g – 30.1 g) were purchased from a certified supplier (Taconic M&B) and used for brain uptake studies. For treatment studies, female and male APP_{ArcSwe} mice (n = 18, weight range: females 22.8 g – 29.4 g, and males 25.9 g – 32.1 g) were selected. This model expresses an Alzheimer's disease (AD)-like A β pathology, containing both the Arctic (APP E693G) and the Swedish (APP KM670/671NL) mutation in the APP gene [53]. Previous research has that neprilysin exhibits higher proteolytic efficiency on A β monomers compared to aggregates [54]. Therefore, 7–8 month-old APP_{ArcSwe} mice were chosen, as at this age they have a higher proportion of soluble A β aggregates compared to A β insoluble plaques, in contrast to older animals [55].

The animals were housed in individually ventilated cages, with 3–5 mice per cage, in an animal facility at Uppsala University. They had free access to food and water, with a controlled environment (humidity: 50–55 %, temperature: 22–23°C) and a 12:12-hour light:dark cycle. All animal experiments were performed in the morning between 8:00–10:00 am. The ethical permit for the study (#5.8.18–20401/2020) was approved by the Uppsala County Animal Ethics Board. All procedures were carried out in compliance with the Swedish ethical on animal experimentation, following the ARRIVE guidelines, and in accordance with the regulations of the Swedish Animal Welfare Agency and complied with the European Communities Council Directive of 22 September 2022 (2010/63/E.U.).

4.2.10. Brain uptake studies and biodistribution in wild-type mice

C57Bl/6JBomTac wild-type mice ($n = 2\text{--}4$ per treatment, total $n = 10$) were administered with an equimolar tracer dose (0.3 nmol/kg body weight, equivalent to 0.05 mg/kg body weight) of ^{125}I -labelled recombinant proteins via intravenous bolus injection into the tail vein. Mice were assigned to experimental groups, which were distributed equally across cages. No randomization or blinding was performed. Two hours post-injection, terminal blood samples were collected while the mice were under deep anaesthesia with isoflurane, and animals were then euthanized by transcardial perfusion with 0.9 % (w/v) NaCl (cat. no. 1.06404.1000, Sigma-Aldrich). Plasma was separated from the blood cells by centrifugation at 10,000 x g for five minutes at 4°C. Perfused brains, along with peripheral organs (liver, spleen, heart, lung, kidney, pancreas, thyroid) and tissues (muscle, bone, skull), were harvested. The radioactivity levels in these samples were measured using a gamma counter (WIZARD 1480, Wallac Oy, Turku, Finland) as previously described [12]. Radioactivity, reported as counts per minute (CPM), was used to quantify the concentrations of the recombinant proteins as percentage of injected dose (%ID) per gram tissue. Statistical analysis was conducted using the ANOVA function in Prism 9 for macOS (version 9.3.1).

4.2.11. Therapeutic study and half-life determination in *APP^{ArcSwe}* mouse model

For therapeutic experiments, equimolar therapeutic doses of recombinant proteins were injected intravenously (bolus) into the tail vein of *APP^{ArcSwe}* mice. The doses were as follows: SST-scFc-scFv8D3 (Mw 84 kDa, 30 nmol/kg bodyweight, 2.5 mg/kg bodyweight, $n = 6$), scFc-scFv8D3 (Mw 82 kDa, 30 nmol/kg bodyweight, 2.5 mg/kg bodyweight, $n = 6$) and PBS ($n = 3$) Only 10 % of the recombinant proteins were labelled with ^{125}I .

Blood samples were collected at time points of 1, 4, 6, 24, 48, 72, and 96 h post-injection using 8 μL glass capillaries (cat. no. 172613, Vitrex Medical A/S) to determine the blood half-life of the injected proteins. After 96 h post-injection, the animals were euthanized by transcardial perfusion with 0.9 % NaCl under deep terminal isoflurane anaesthesia.

Peripheral organs (liver, spleen, heart, lung, kidney, pancreas, thyroid), tissues (muscle, bone, skull), and blood were harvested. Plasma was separated from the blood cells by centrifugation at 10,000 x g for five minutes at 4°C. The brain was dissected into two hemispheres, and the left hemisphere was further subdivided into the following regions: (1) hippocampal area, (2) rest of cerebrum, and (3) cerebellum. Radioactivity levels in the blood samples, brain regions, and organs were measured using a Wizard 2470 gamma counter (Perkin Elmer Inc., Waltham, USA) as previously described [12]. The concentration of radioactivity in these tissues and blood samples (measured as counts per minute, CPM) was calculated as percentage of injected dose (%ID) per gram tissue or blood.

To analyse the ratio of [^{125}I]-labelled recombinant proteins to free ^{125}I , plasma and urine samples were subjected to thin layer chromatography (TLC). Briefly, 2 μL of each sample was applied to a baseline on a silica-coated aluminum plate (cat. no. 105554001, Merck) and allowed to air-dry. The TLC plate was then placed in a separation chamber

containing 70 % acetone as a mobile phase. Once the solvent front had migrated approximately two-thirds of the length of the plate, the plate was removed and dried. Radioactivity was visualised using a Cyclone PhosphorImager (Perkin Elmer)

4.2.12. Sample preparation of brain and organs from therapeutic study

The right hemisphere of the brain was preserved intact and stored at -80°C , while the left hemisphere was used for homogenization to obtain different populations of A β . The left hemisphere was subdivided into the following regions: (1) hippocampal area, (2) rest of cerebrum, and (3) cerebellum. The tissue was weighed and diluted at a ratio of 1:5 (w/v) with tris-buffered saline (TBS) containing cOMplete™ protease inhibitors (cat. no. 11697498001, Roche) in soft tissue homogenizing tubes (cat. no. 19–627 and 19–626–3, Revvity). Homogenization was performed using a Precellys Evolution System (Bertin Corp, Rockville, MD, USA). The homogenates were then centrifuged at 16,000 x g for one hour at 4°C to generate a soluble A β extract from the brain. The remaining pellet was re-homogenized with TBS containing 1 % Triton-X (TBST, cat. no. T8787, Sigma-Aldrich) and centrifuged again at 16,000 x g for one hour at 4 °C to generate a membrane-bound soluble A β extract. Finally, the remaining pellet was homogenized with 70 % formic acid (FA, cat. no. F0507, Sigma-Aldrich) and centrifuged at 16,000 x g at for one hour at 4°C to generate an insoluble A β brain extract. The formic acid samples were initially neutralized with 2 M Tris pH8.0 and further diluted with ELISA incubation buffer (1 x PBS with 0.1 % BSA and 0.05 % Tween-20). The resulting brain extracts were stored at -80°C until further use.

4.2.13. Neprilysin protein-levels ELISA

The levels of neprilysin in both the TBS soluble fractions and TBST membrane-bound soluble fraction from brain and kidney samples were measured using a neprilysin ELISA kit (cat. no. DY1126, R&D), following the manufacturer's protocol. Ninety-six well half-area plates (cat. no. 3960, Corning Incorporated) were coated with 1.6 $\mu\text{g}/\text{mL}$ of the capture antibody (Goat-anti mouse neprilysin) in PBS overnight at 4°C. The following day, the plates were blocked with 1 % BSA in 1 x PBS for two hours at RT. Samples were diluted 1:10 (v/v) in ELISA incubation buffer (1 x PBS with 0.1 % BSA and 0.05 % Tween-20) and incubated for two hours at RT. Afterwards, biotinylated goat anti-mouse neprilysin detection antibody (final concentration: 400 ng/mL) was added, and the plates were incubated for an additional two hours at RT. The final incubation was performed using Streptavidin-HRP, diluted 1:4000 (v/v) (cat. no. 3310–9–1000, Mabtech) for one hour at RT. The signal was developed using K-blue aqueous TMB (cat. no. 331177, Neogen Corp). The absorbance was measured at 450 nm using a Spark® multimode microplate reader (Tecan, Männedorf, Switzerland). Wells were washed with ELISA washing buffer (1 x PBS with 0.05 % Tween-20) between each step after blocking.

4.2.14. A β ELISA

For the analysis of A β , indirect sandwich ELISA's were performed. Ninety-six-well half-area plates (cat. no. 3690, Corning Inc.) were coated with 1 $\mu\text{g}/\text{mL}$ capture antibody (details provided in table below) for overnight at 4°C. Following this, plates were incubated for two hours at RT with 1 % BSA in PBS for blocking. Brain homogenates (TBS and TBST) were diluted 1:10 (v/v) in ELISA incubation buffer (EIB, 0.1 % BSA, 0.05 % Tween-20 in PBS), whereas the FA fraction was diluted 1:3000 (v/v) in ELISA incubation buffer and applied in duplicates for overnight at 4°C. An in-house produced biotinylated 3D6 antibody was used for most ELISA set-ups at a final concentration of 1 $\mu\text{g}/\text{mL}$ in ELISA incubation buffer followed by a two hours incubation at RT. For detection, streptavidin-HRP (cat. no. 3310–9–1000, Mabtech) was diluted 1:4000 (v/v) in EIB. Signal was developed with K-blue aqueous TMB (cat. no. 331177, Neogen Corp) and stopped with 1 M H_2SO_4 (cat. no. 35347, Fisher Scientific) in a 1:1 (v/v) ratio. Absorbance was measured at 450 nm using a Spark® multimode microplate reader

(Tecan, Männedorf, Switzerland). Wells were washed with ELISA washing buffer (1 x PBS with 0.05 % Tween-20) between each step after blocking.

ELISA description	Figure	Capture antibody	Detection antibody
“A β 42 monomers and aggregates with C- and N-terminal available”	4	A β 1 – 42 recombinant rabbit monoclonal antibody (H31L21) binds to A β C-terminal part (cat. no. 700254, Thermo Fisher)	3D6 -biotinylated, in house produced
“A β dimers, oligomers and aggregates, N-terminal available”	5	3D6, in house produced [56], monoclonal, binds A β N-terminus, recognizes monomers and aggregates	3D6 -biotinylated, in house produced
“A β hairpin (A11) and N-terminal available”	6	Oligomer A11 rabbit polyclonal antibody, recognizes ab oligomeric species of amyloidogenic polypeptides (cat. no. AHB0052, Thermo Fisher)	3D6 -biotinylated, in house produced
“monomeric A β ”	7 & Supplementary Figure 5	m266, in house produced [40] binds to mid-region, specific for monomers	3D6 -biotinylated, in house produced

4.3. Statistical analysis

Data are presented as mean \pm SD. Statistical significance was determined using either an unpaired *t*-test or one-way ANOVA followed by Bonferroni’s post-hoc analysis. *p*-values were considered significant at *: *p* < 0.05, **: *p* < 0.01, ***: *p* < 0.001.

Authors’ contributions

GH and NGM designed the project. AN, AG and NGM produced the proteins. NGM, FR and AG performed the in vitro assays. NGM, FR, AC, AP and SS performed in vivo work. NGM and GH analyzed the results. GH and NGM wrote the manuscript with valuable input from all the co-authors. The authors read and approved the final manuscript.

CRedit authorship contribution statement

Nicole G. Metzendorf: Writing – review & editing, Writing – original draft, Visualization, Validation, Project administration, Methodology, Data curation. **Ana Goddec:** Methodology. **Greta Hultqvist:** Writing – review & editing, Writing – original draft, Supervision, Resources, Funding acquisition, Conceptualization. **Fadi Rofo:** Methodology, Investigation. **Aikaterini Chourlia:** Methodology. **Alex Petrovic:** Methodology. **Stina Syvänen:** Resources, Methodology. **Antonino Napoleone:** Methodology.

Consent for publication

Not applicable

Ethics approval and consent to participate

The ethical permit was approved by the Uppsala County Animal Ethics Board (# 5.8.18–04903–2022). No human data is included in the manuscript. All authors approve the publication.

Funding

This work was supported by grants from Swedish Research Council (2021–01083, 2019–01883, 2023–01883), Åhlén-stiftelsen, Magnus Bergvalls stiftelse, Vinnova (2021–02640), Alzheimerfonden, Stiftelsen Olle Engkvist Byggmästare, Parkinsonfonden, Bissen Brainwalk, Hjärnfonden FO2024–0243, O.E. och Edla Johanssons vetenskapliga stiftelse and Torsten Söderbergs stiftelse.

Declaration of Competing Interest

The authors declare no competing interests.

Acknowledgements

We thank the Biophysical Screening and Characterization Unit at SciLifeLab for the use of the Tycho NT.6 instrument. Radiochemistry and animal work were conducted at the SciLifeLab Pilot Facility for Pre-clinical PET-MRI, Uppsala University, Sweden, funded by the Knut and Alice Wallenberg Foundation. We also express our gratitude to Farahnaz Ranjbarian and Anders Hofer from the Department of Medical Biochemistry and Biophysics at Umeå University for performing mass photometry (Refeyn) on our samples. Figures were created using Bio-render.com. The authors declare no competing interests.

Appendix A. Supporting information

Supplementary data associated with this article can be found in the online version at [doi:10.1016/j.biopha.2025.118325](https://doi.org/10.1016/j.biopha.2025.118325).

Data availability

Data is provided within the manuscript or [supplementary information](#) files. Possible additional data are available to the corresponding author upon reasonable request.

References

- [1] Y. Yu, Y. Gao, B. Winblad, L.O. Tjernberg, S. Schedin-Weiss, A super-resolved view of the alzheimer’s disease-related amyloidogenic pathway in hippocampal neurons, *J. Alzheimers Dis.* 83 (2021) 833–852.
- [2] D.-S. Wang, D.W. Dickson, J.S. Malter, β -amyloid degradation and alzheimer’s disease, *J. Biomed. Biotechnol.* 2006 (2006) 58406.
- [3] T. Saïdo, M.A. Leissring, Proteolytic degradation of amyloid β -protein, *Cold Spring Harb. Perspect. Med.* 2 (2012) a006379.
- [4] J. Żukowska, S.J. Moss, V. Subramanian, K.R. Acharya, Molecular basis of selective amyloid- β degrading enzymes in Alzheimer’s disease, *FEBS J.* 291 (2024) 2999–3029.
- [5] K. Shirotani, et al., Neprilysin Degrades Both Amyloid β Peptides 1–40 and 1–42 Most Rapidly and Efficiently among Thiorphan- and Phosphoramidon-sensitive Endopeptidases, *J. Biol. Chem.* 276 (2001) 21895–21901.
- [6] Y. Takaki, et al., Biochemical Identification of the Neutral Endopeptidase Family Member Responsible for the Catabolism of Amyloid β Peptide in the Brain1, *J. Biochem. (Tokyo)* 128 (2000) 897–902.
- [7] J.S. Miners, et al., Abeta-degrading enzymes in Alzheimer’s disease, *Brain Pathol. Zur. Switz.* 18 (2008) 240–252.
- [8] E.R.L.C. Vardy, A.J. Catto, N.M. Hooper, Proteolytic mechanisms in amyloid-beta metabolism: therapeutic implications for Alzheimer’s disease, *Trends Mol. Med.* 11 (2005) 464–472.
- [9] L.B. Hersh, D.W. Rodgers, Neprilysin and amyloid beta peptide degradation, *Curr. Alzheimer Res.* 5 (2008) 225–231.
- [10] S. Fukami, et al., A β -degrading endopeptidase, neprilysin, in mouse brain: synaptic and axonal localization inversely correlating with A β pathology, *Neurosci. Res.* 43 (2002) 39–56.
- [11] N. Iwata, et al., Global brain delivery of neprilysin gene by intravascular administration of AAV vector in mice, *Sci. Rep.* 3 (2013) 1472.
- [12] F. Rofo, et al., Enhanced neprilysin-mediated degradation of hippocampal A β 42 with a somatostatin peptide that enters the brain, *Theranostics* 11 (2021) 789–804.
- [13] N. Iwata, et al., Identification of the major A β 1–42-degrading catabolic pathway in brain parenchyma: Suppression leads to biochemical and pathological deposition, *Nat. Med.* 6 (2000) 143–150.
- [14] R. Madani, et al., Lack of neprilysin suffices to generate murine amyloid-like deposits in the brain and behavioral deficit in vivo, *J. Neurosci. Res.* 84 (2006) 1871–1878.

- [15] S.-M. Huang, et al., Nephrylysin-sensitive synapse-associated amyloid- β peptide oligomers impair neuronal plasticity and cognitive function *, *J. Biol. Chem.* 281 (2006) 17941–17951.
- [16] K. Yasojima, H. Akiyama, E.G. McGeer, P.L. McGeer, Reduced neprilysin in high plaque areas of Alzheimer brain: a possible relationship to deficient degradation of β -amyloid peptide, *Neurosci. Lett.* 297 (2001) 97–100.
- [17] S. Wang, et al., Expression and functional profiling of neprilysin, insulin degrading enzyme and endothelin converting enzyme in prospectively studied elderly and Alzheimer's brain, *J. Neurochem.* 115 (2010) 47–57.
- [18] N. Iwata, Y. Takaki, S. Fukami, S. Tsubuki, T.C. Saido, Region-specific reduction of A β -degrading endopeptidase, neprilysin, in mouse hippocampus upon aging, *J. Neurosci. Res.* 70 (2002) 493–500.
- [19] A. Sandberg, et al., Stabilization of neurotoxic Alzheimer amyloid- β oligomers by protein engineering, *Proc. Natl. Acad. Sci. U. S. A.* 107 (2010) 15595–15600.
- [20] S.M. Ruttenberg, J.S. Nowick, A turn for the worse: A β β -hairpins in Alzheimer's disease, *Bioorg. Med. Chem.* 105 (2024) 117715.
- [21] C. Nilsberth, et al., The 'Arctic' APP mutation (E693G) causes Alzheimer's disease by enhanced A β protofibril formation, *Nat. Neurosci.* 4 (2001) 887–893.
- [22] T. Saito, et al., Somatostatin regulates brain amyloid β peptide A β 42 through modulation of proteolytic degradation, *Nat. Med.* 11 (2005) 434–439.
- [23] D. Saiz-Sanchez, et al., Somatostatin, olfaction, and neurodegeneration, *Front. Neurosci.* 14 (2020).
- [24] P. Davies, R. Katzman, R.D. Terry, Reduced somatostatin-like immunoreactivity in cerebral cortex from cases of Alzheimer disease and Alzheimer senile dementia, *Nature* 288 (1980) 279–280.
- [25] K. Sandoval, D. Umbaugh, A. House, A. Crider, K. Witt, Somatostatin receptor subtype-4 regulates mRNA expression of amyloid-beta degrading enzymes and microglia mediators of phagocytosis in brains of 3xTg-AD mice, *Neurochem. Res.* 44 (2019) 2670–2680.
- [26] A. Shi, A.L. Petrache, J. Shi, A.B. Ali, Preserved calretinin interneurons in an app model of alzheimer's disease disrupt hippocampal inhibition via upregulated P2Y1 purinoreceptors, *Cereb. Cortex* 30 (2020) 1272–1290.
- [27] H. Soler, et al., The GABAergic septohippocampal connection is impaired in a mouse model of tauopathy, *Neurobiol. Aging* 49 (2017) 40–51.
- [28] G. Hultqvist, S. Syvänen, X.T. Fang, L. Lannfelt, D. Sehlin, Bivalent brain shuttle increases antibody uptake by monovalent binding to the transferrin receptor, *Theranostics* 7 (2017) 308–318.
- [29] D. Sehlin, et al., Antibody-based PET imaging of amyloid beta in mouse models of Alzheimer's disease, *Nat. Commun.* 7 (2016) 10759.
- [30] Y.J.Y. Zuchero, et al., Discovery of novel blood-brain barrier targets to enhance brain uptake of therapeutic antibodies, *Neuron* 89 (2016) 70–82.
- [31] W.M. Pardridge, Blood–brain barrier drug delivery of IgG fusion proteins with a transferrin receptor monoclonal antibody, *Expert Opin. Drug Deliv.* 12 (2015) 207–222.
- [32] F. Rofo, et al., Wide-ranging effects on the brain proteome in a transgenic mouse model of alzheimer's disease following treatment with a brain-targeting somatostatin peptide, *ACS Chem. Neurosci.* (2021), <https://doi.org/10.1021/acscchemneuro.1c00303>.
- [33] S. Tsubuki, Y. Takai, T.C. Saido, Dutch, flemish, italian, and arctic mutations of APP and resistance of A β to physiologically relevant proteolytic degradation, *Lancet* 361 (2003) 1957–1958.
- [34] F. Rofo, et al., Blood–brain barrier penetrating neprilysin degrades monomeric amyloid-beta in a mouse model of Alzheimer's disease, *Alzheimers Res. Ther.* 14 (2022) 180.
- [35] J.I. Morrison, N.G. Metzendorf, F. Rofo, A. Petrovic, G. Hultqvist, A single-chain fragment constant design enables easy production of a monovalent blood-brain barrier transporter and provides an improved brain uptake at elevated doses, *J. Neurochem.* (2023), <https://doi.org/10.1111/jnc.15768>.
- [36] A. de la Rosa, et al., Introducing or removing heparan sulfate binding sites does not alter brain uptake of the blood–brain barrier shuttle scFv8D3, *Sci. Rep.* 12 (2022) 1–17.
- [37] S. Syvänen, et al., Efficient clearance of A β protofibrils in A β PP-transgenic mice treated with a brain-penetrating bifunctional antibody, *Alzheimers Res. Ther.* 10 (2018) 49.
- [38] R. Faresjö, et al., Brain pharmacokinetics of two BBB penetrating bispecific antibodies of different size, *Fluids Barriers CNS* 18 (2021) 26.
- [39] Metzendorf, N.G., Sehlin, D. & Hultqvist, G. ELISA quantification of different types of amyloid-beta in tissue extracts. (2024).
- [40] R.B. DeMattos, et al., Peripheral anti-A β antibody alters CNS and plasma A β clearance and decreases brain A β burden in a mouse model of Alzheimer's disease, *Proc. Natl. Acad. Sci. U. S. A.* 98 (2001) 8850–8855.
- [41] Z. Fu, W.E. Van Nostrand, S.O. Smith, Anti-parallel β -hairpin structure in soluble A β oligomers of A β 40-Dutch and A β 40-Iowa, *Int. J. Mol. Sci.* 22 (2021) 1225.
- [42] W. Hoyer, C. Grönwall, A. Jonsson, S. Ståhl, T. Härd, Stabilization of a β -hairpin in monomeric Alzheimer's amyloid- β peptide inhibits amyloid formation, *Proc. Natl. Acad. Sci.* 105 (2008) 5099–5104.
- [43] C.G. Glabe, Structural classification of toxic amyloid oligomers *, *J. Biol. Chem.* 283 (2008) 29639–29643.
- [44] D.J. Lindberg, E. Wesén, J. Björkeröth, S. Rocha, E.K. Esbjörner, Lipid membranes catalyse the fibril formation of the amyloid- β (1–42) peptide through lipid-fibril interactions that reinforce secondary pathways, *Biochim. Biophys. Acta BBA Biomembr.* 1859 (2017) 1921–1929.
- [45] S. Banerjee, M. Hashemi, K. Zagorski, Y.L. Lyubchenko, Interaction of A β 42 with membranes triggers the self-assembly into oligomers, *Int. J. Mol. Sci.* 21 (2020) 1129.
- [46] J. Yang, et al., Differentiating A β 40 and A β 42 in amyloid plaques with a small molecule fluorescence probe, *Chem. Sci.* 11 (2020) 5238–5245.
- [47] R.J. Boado, Y. Zhang, Y. Wang, W.M. Pardridge, Engineering and expression of a chimeric transferrin receptor monoclonal antibody for blood-brain barrier delivery in the mouse, *Biotechnol. Bioeng.* 102 (2009) 1251–1258.
- [48] X.T. Fang, D. Sehlin, L. Lannfelt, S. Syvänen, G. Hultqvist, Efficient and inexpensive transient expression of multispecific multivalent antibodies in Expi293 cells, *Biol. Proced. Online* 19 (2017).
- [49] G. Young, et al., Quantitative mass imaging of single molecules, *Science* 360 (2018) 423–427.
- [50] N. Kakiya, et al., Cell Surface Expression of the Major Amyloid- Peptide (A)-degrading Enzyme, Nephrylysin, Depends on Phosphorylation by Mitogen-activated Protein Kinase/Extracellular Signal-regulated Kinase Kinase (MEK) and Dephosphorylation by Protein Phosphatase, 1a. *J. Biol. Chem.* 287 (2012) 29362–29372.
- [51] F. Rofo, et al., Novel multivalent design of a monoclonal antibody improves binding strength to soluble aggregates of amyloid beta, *Transl. Neurodegener.* 10 (2021) 38.
- [52] F.C. Greenwood, W.M. Hunter, J.S. Glover, The preparation of 131I-labelled human growth hormone of high specific radioactivity, *Biochem. J.* 89 (1963) 114–123.
- [53] A. Lord, et al., The Arctic Alzheimer mutation facilitates early intraneuronal A β aggregation and senile plaque formation in transgenic mice, *Neurobiol. Aging* 27 (2006) 67–77.
- [54] M.A. Leissring, et al., Enhanced proteolysis of beta-amyloid in APP transgenic mice prevents plaque formation, secondary pathology, and premature death, *Neuron* 40 (2003) 1087–1093.
- [55] A. Lord, et al., Amyloid-beta protofibril levels correlate with spatial learning in Arctic Alzheimer's disease transgenic mice, *FEBS J.* 276 (2009) 995–1006.
- [56] K. Johnson-Wood, et al., Amyloid precursor protein processing and A beta42 deposition in a transgenic mouse model of Alzheimer disease, *Proc. Natl. Acad. Sci. U. S. A.* 94 (1997) 1550–1555.